JACS
JOURNAL OF THE AMERICAN CHEMICAL SOCIETY

Article

pubs.acs.org/JACS

Efficient Isotope Editing of Proteins for Site-Directed Vibrational Spectroscopy

Sebastian Peuker,*[,†] Hanna Andersson,[†] Emil Gustavsson,[†] Kiran Sankar Maiti,[†] Rafal Kania,[†] Alavi Karim,[†] Stephan Niebling,[†] Anders Pedersen,[‡] Mate Erdelyi,[†] and Sebastian Westenhoff*[,†]

[†]Department of Chemistry and Molecular Biology, University of Gothenburg, SE-405 30 Gothenburg, Sweden
[‡]Swedish NMR Centre at the University of Gothenburg, P.O. Box 465, SE-405 30 Gothenburg, Sweden

Supporting Information

ABSTRACT: Vibrational spectra contain unique information on protein structure and dynamics. However, this information is often obscured by spectral congestion, and site-selective information is not available. In principle, sites of interest can be spectrally identified by isotope shifts, but site-specific isotope labeling of proteins is today possible only for favorable amino acids or with prohibitively low yields. Here we present an efficient cell-free expression system for the site-specific incorporation of any isotope-labeled amino acid into proteins. We synthesized 1.6 mg of green fluorescent protein with an isotope-labeled tyrosine from 100 mL of cell-free reaction extract. We unambiguously identified spectral features of the tyrosine in the fingerprint region of the time-resolved infrared absorption spectra. Kinetic analysis confirmed the existence of an intermediate state between photoexcitation and proton transfer that lives for 3 ps. Our method lifts vibrational spectroscopy of proteins to a higher level of structural specificity.

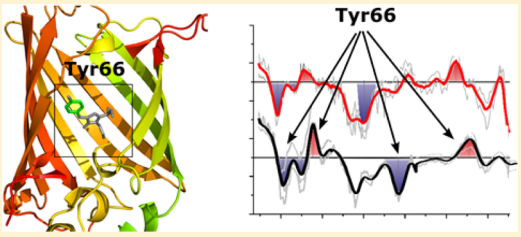

INTRODUCTION

Proteins are in constant motion, and their diverse functions are ultimately governed by this dynamic character.[1,2] Methods to study protein structural dynamics are in demand. Vibrational spectroscopy is a very powerful means to probe the conformational changes of chemical entities.[3] A number of time-resolved and multidimensional infrared spectroscopic techniques have been developed, and they can be used to directly monitor vibrational coupling of chemical groups in a time-resolved manner.[4−8] Unfortunately, vibrational spectra of proteins are crowded. The assignment of spectral features to specific sites is at best tedious but most often impossible. This seriously restricts the application of vibrational spectroscopy to study protein dynamics.

A strategy to overcome the crowdedness of the spectra is to label specific sites of interest in the protein. It is often possible to label cofactors or ligands.[8,9] Moreover, infrared-active reporter groups can be attached to the proteins after protein expression[10] by introducing unnatural amino acids with infrared-active functional groups during protein synthesis[11−16] or by introducing isotope-edited amino acids.[17−22] Using infrared-active reporter groups has the advantage that they are typically easily identified in the spectra. These approaches have yielded remarkable insight into the rearrangements of secondary structure[13] and the solubilization of proteins,[10] for example. The latter method, labeling with isotopes, ensures that the chemical properties of the proteins remain unaltered. This gives the method a distinct advantage over labeling with reporter groups, as it allows monitoring of active sites that directly participate in the enzymatic activity of the protein.

The increased mass of the isotopes causes chemical bonds to oscillate at lower frequencies, which is observed as red-shifted peaks in the vibrational spectra.[23] Infrared spectroscopy of isotope-labeled proteins has yielded unique insights into the folding dynamics of model peptides[19,20] and amyloid fibers,[17] was used to solve the three-dimensional dimer arrangement of a membrane-bound α-helical protein,[24] and has helped to elucidate the photocycle of membrane proton pumps.[25]

Today, the wider-spread application of site-specific isotope labeling is restricted by protein synthesis. Most of the studies mentioned involved proteins that were produced by chemical peptide synthesis.[17,19,20,24] This is a versatile method for site-specific insertion of isotope-labeled amino acids into proteins; however, it is also restricted to short peptide chains. Nevertheless, some proteins can be labeled site-selectively by connecting a chemically produced peptide chain to a truncated version of the protein.[21] In in vivo expression systems, site-specific isotope labeling is possible when an amino acid occurs only a single time in a polypeptide chain and an expression host that is auxotrophic for that amino acid is available.[25,26]

With in vitro expression systems,[26] tyrosines can be labeled as a result of the existence of an orthogonal tRNA/aminoacyl transferase pair in *Escherichia coli*.[25,27] The most general in vitro method is to introduce unnatural amino acids in response to an amber stop codon with chemically aminoacylated suppressor tRNA.[28,29] This strategy makes possible the incorporation of any amino acid, but it has not yet been used for infrared spectroscopic studies,[30] presumably because of the moderate

Received: December 14, 2015
Published: January 21, 2016

DOI: 10.1021/jacs.5b12680
J. Am. Chem. Soc. 2016, 138, 2312−2318

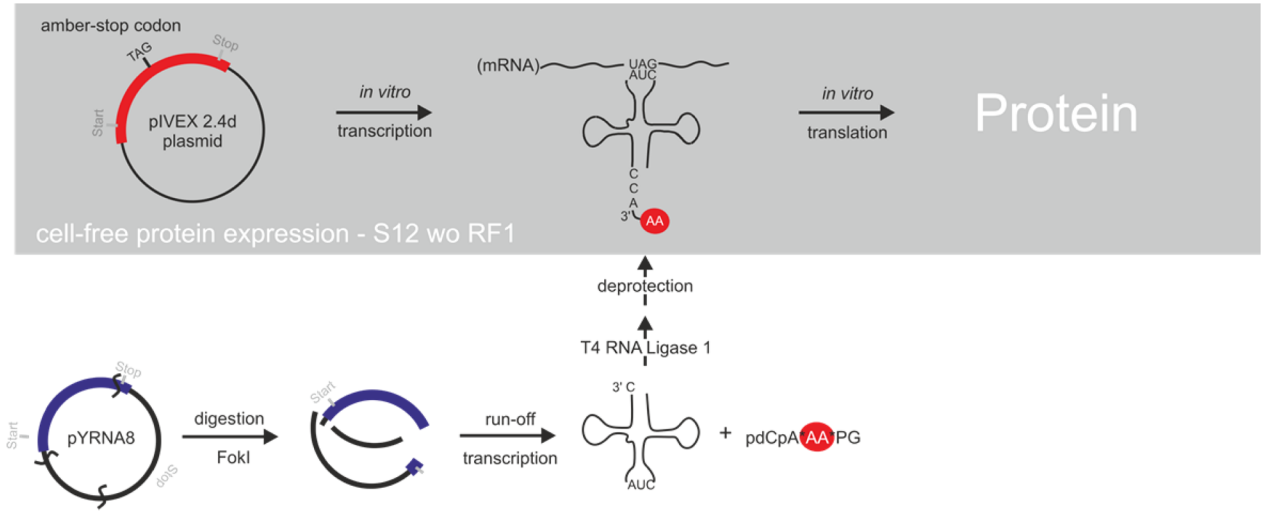

Figure 1. Site-directed introduction of isotope-labeled amino acids into proteins. Shown is a scheme of the experimental principle applied to synthesize isotope-labeled proteins. Details are given in the main text. Abbreviations: AA, amino acid; RF1, release factor 1; PG, protection group; pdCpA, 5′-*O*-phosphoryl-2′-deoxycytidylyl-(3′→5′)adenosine.

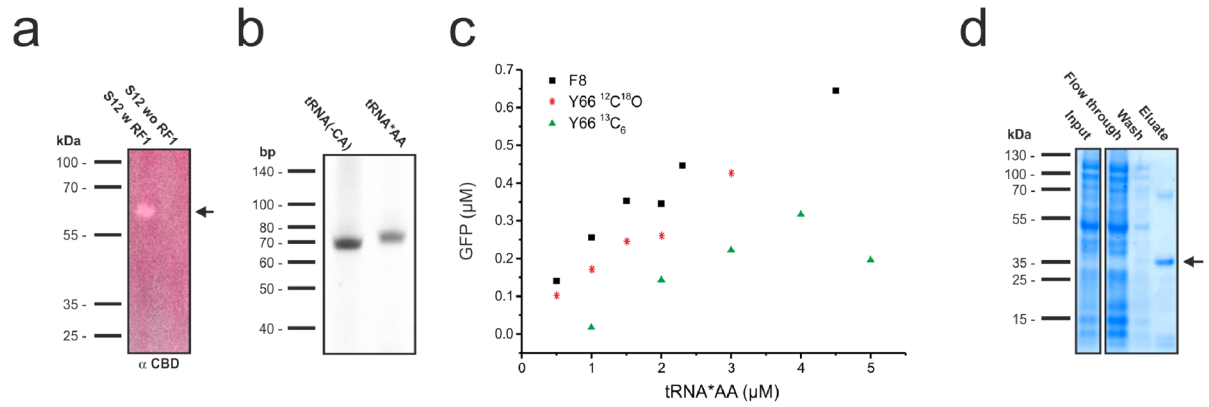

Figure 2. Characterization of the site-directed labeling procedure. (a) Verification of RF1 removal by Western blotting. RF1 was detected by an antichitin binding domain antibody (α CBD). The apparent molecular weight of RF1−$(CBD)_3$ is 69.9 kDa. (b) Verification of the products of the runoff transcription and ligation by a 10% Novex TBE-Urea gel stained with SybrSafe. The lengths of tRNA(-CA) and tRNA*AA are 74 and 76 bases, respectively. (c) Test of the suppression efficacies of $tRNA^{Phe}_{CUA}$ and of $tRNA^{Tyr\text{-}^{12}C^{18}O}_{CUA}$ and $tRNA^{Tyr\text{-}^{13}C_6}_{CUA}$ by cell-free expression of $GFP^{Phe8TAG}$ and $GFP^{Tyr66TAG}$, respectively. Expression of GFP was quantified by means of fluorescence. (d) SDS-PAGE of the purification of GFP using $tRNA^{Tyr\text{-}^{13}C_6}_{CUA}$ by Ni-affinity chromatography. The apparent molecular weight of GFP is 29.8 kDa.

protein production yields. Fundamentally limiting the yield is release factor 1 (RF1), which competes with the suppressor tRNA for the amber stop codon. This problem has recently been addressed in a modified *E. coli* strain developed by the Otting group.[31] The reaction mixture from this strain can be reliably depleted of RF1 by affinity chromatography.

Here we combine the two approaches for in vitro expression. We explore two strategies for the synthesis of chemically aminoacylated suppressor tRNA and outline routes for the incorporation of all native amino acids. Finally, we develop a simplified procedure for $^{18}O^{13}C$-labeled amino acids from ^{13}C precursors, which is of particular practical importance for infrared spectroscopy. Combined, we were able to produce milligram quantities of site-specifically isotope-labeled proteins. Using this strategy, we assigned vibrations of a key tyrosine in the active site of green fluorescent protein (GFP) to peaks in the infrared fingerprint spectral region.

RESULTS

In the following sections, the three major components of the method are described: the cell-free expression system, the synthesis of the chemically aminoacylated suppressor $tRNA^{AA}_{CUA}$, and the synthesis of isotope-labeled and appropriately protected amino acids. The final section describes how isotope-labeled GFP was used to assign chromophore vibrations in UV pump−infrared probe spectra. Figure 1 provides an overview of the synthesis.

Cell-Free Expression System. We used a cell-free protein expression system in batch mode.[32,33] In order to maximize the incorporation efficiency of the modified amino acids, the S12 extract was produced from a genomically modified *E. coli* strain BL21 Star (DE3):RF1-CBD3 developed by Otting and co-workers.[31] This strain allows the removal of RF1 by means of affinity chromatography. With this, the termination of the translation is avoided when the stop codon is reached.[34] The complete removal of RF1 from the S12 extract was confirmed

DOI: 10.1021/jacs.5b12680
J. Am. Chem. Soc. 2016, 138, 2312−2318

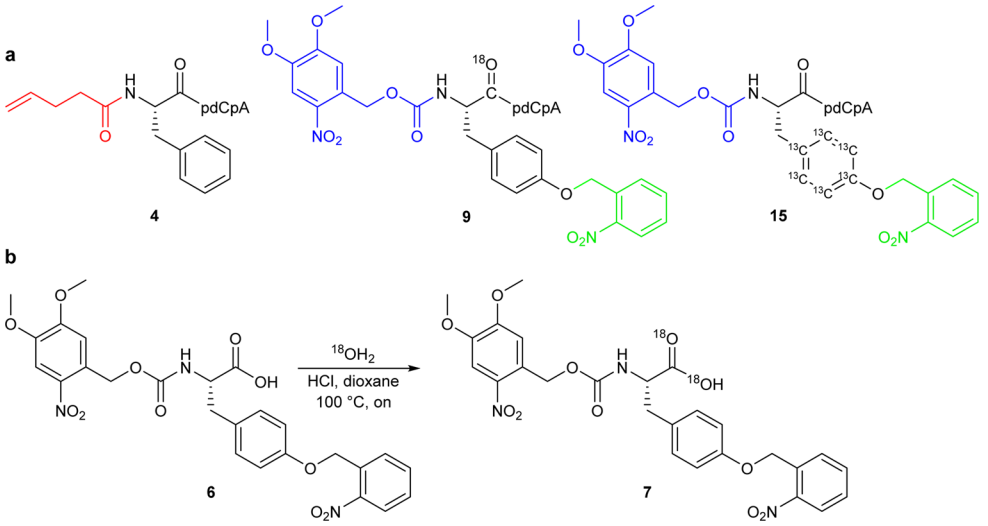

Figure 3. Chemical intermediates in the preparation of aminoacyl-tRNAs. (a) Aminoacylated dinucleotide derivatives **4**, **9**, and **15** were synthesized (Supplementary Schemes 1−3) and used in the preparation of tRNAs for site-specific incorporation into GFP. The iodine-labile 4-PO protecting group (red) was used for phenylalanine derivative **4**, while the photolabile protecting groups NVOC (blue) and NB (green) were used for tyrosine derivatives **9** and **15**, respectively. (b) Simplified procedure for ^{18}O labeling of carboxylic acids (e.g., amino acid derivative **6**) utilizing ^{18}O-enriched water, 1,4-dioxane, and commercially available 4 M HCl in 1,4-dioxane as an acid source (Supplementary Scheme 2).

by Western blotting (Figure 2a), and the expression yield of the modified extract was 75 μg of protein/mL of reaction mixture.

Synthesis of the Chemically Aminoacylated Suppressor tRNA$^{AA}_{CUA}$. Chemically aminoacylated tRNA(-CA)$^{AA}_{CUA}$ was synthesized by enzymatically ligating 3′-truncated tRNA(-CA)$_{CUA}$ with aminoacyl-pdCpA (synthesized as described below) in vitro using T4 RNA ligase 1 (Figure 2b).[35,36] The precursor, 3′-truncated tRNA(-CA)$_{CUA}$, was prepared by runoff transcription from FokI-digested template DNA (pYRNA8) (Figure 2b, left lane), and complete digestion was observed using 0.25 unit of FokI/μg of pYRNA8 in 15 min. As judged by a 10% TBE urea gel, the ligation of aminoacyl-pdCpA to tRNA(-CA)$_{CUA}$ was quantitative (Figure 2b, right lane).

We tested the efficiency of this system by the expression of GFP. The level of fluorescence is directly proportional to the level of functional full-length protein. We incorporated a phenylalanine at position 8 and a tyrosine at position 66 by expression of GFP from GFPcyc3^{Phe8TAG} and GFPcyc3^{Tyr66TAG} templates, respectively. Figure 2c shows that the level of expressed GFP scaled with the concentration of the respective tRNA$^{AA}_{CUA}$. The level of expressed GFP scaled equally for the F8 and Y66 labeled with Tyr-$^{12}C^{18}O$, but the incorporation was lower for Y66 labeled with Tyr-$^{13}C_6$. We attribute this difference to nonoptimal deprotection of the particular batch of tRNA$^{Tyr\text{-}^{13}C_6}_{CUA}$. Up to 30% of the tRNA$^{AA}_{CUA}$ was translated into proteins.

Synthesis of Aminoacyl-pdCpAs. Aminoacylated dinucleotide derivatives (aminoacyl-pdCpAs) were synthesized by aminoacylation of pdCpA with the desired amino acid (Figure 1).[35] To prevent side reactions and to increase the stability of the amino acid−nucleotide ester linkage, the α-amino and side-chain functional groups were protected. We explored two protecting group strategies.[37] The iodine-labile 4-pentenoyl (4-PO) group was used as an α-amino protecting group in the preparation of phenylalanyl-pdCpA (**4**) (Figure 3a and Supplementary Scheme 1). It is ideal for amino acids without side-chain functionality (Table 1)[38] but can also be applied in orthogonal protecting strategies, e.g., together with photolabile side-chain protecting groups. However, it is unsuitable for amino acids having oxidizable side chains. Tyrosine falls into this category, and therefore, the photolabile 6-nitroveratryloxycarbonyl (NVOC) and 2-nitrobenzyl (NB) groups were used as α-amino and side-chain protecting groups in the synthesis of tyrosinyl-pdCpA (**9** and **15**, respectively) (Figure 3a and Supplementary Schemes 2 and 3). 6-Nitroveratryl (NV) is a possible substitute for NB, and Table 1 summarizes suitable protection strategies for all of the natural amino acids. Compound **4** was produced in an overall yield of 21% starting from L-phenylalanine, and **9** and **15** were produced in overall yields of 4% and 6% starting from commercially available L-tyrosine and L-[*phenyl*-$^{13}C_6$]tyrosine, respectively.

Table 1. Overview of the Most Common Amino Acid Protecting Group Strategies Applicable for the Preparation of Chemically Aminoacylated tRNAs

Protecting group strategy		
α-amine	side chain	Examples of natural amino acids
4-PO	–	nonpolar: Gly, Ala, Val, Leu, Ile, Met, Pro, Phe
		polar basic: Arg
4-PO	NV/NB	polar: Ser, Thr, Asn, Gln
		polar acidic: Asp, Glu
4-PO	NVOC	polar basic: Lys
NVOC	–	nonpolar: Gly, Ala, Val, Leu, Ile, Met, Pro, Phe, Trp
		polar basic: Arg
NVOC	NV/NB	polar: Ser, Thr, Cys, Asn, Gln, Tyr
		polar acidic: Asp, Glu
		polar basic: His
NVOC	NVOC	polar basic: Lys

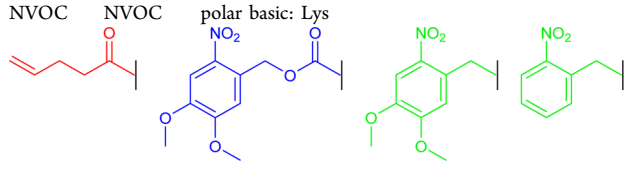

DOI: 10.1021/jacs.5b12680
J. Am. Chem. Soc. 2016, 138, 2312−2318

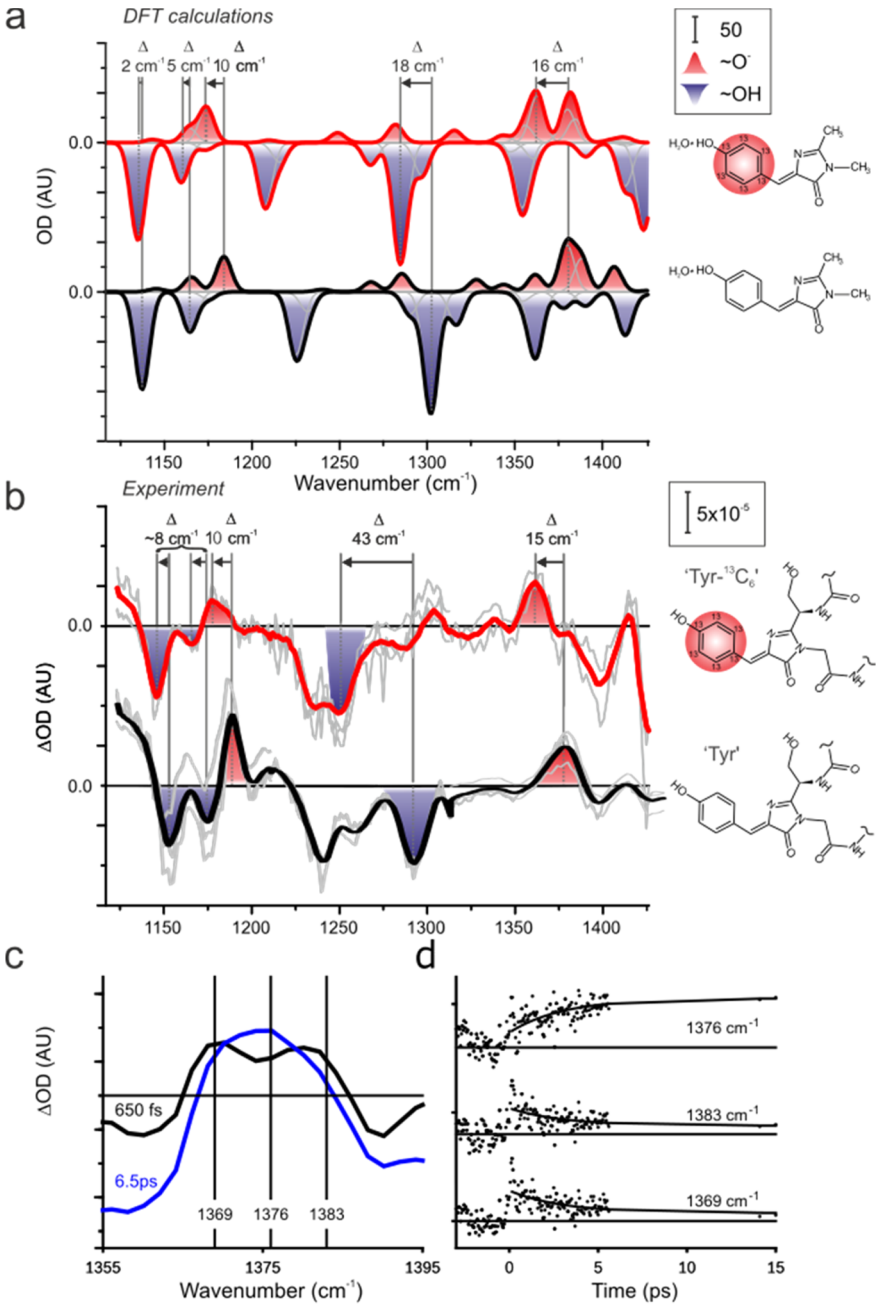

Figure 4. UV pump−infrared probe spectra of GFP$^{Tyr66\text{-}^{13}C_6}$. (a) DFT calculations of infrared absorption spectra of model compounds representing the chromophore of GFP as illustrated. The isotope-labeled part of the molecule is highlighted. The single modes underlying the spectra shown in gray are plotted as Gaussian functions with a full width at half-maximum of 10 cm^{-1}. (b) UV pump−infrared probe spectra of wild-type GFP (black) and GFP$^{Tyr66\text{-}^{13}C_6}$ (red). Three spectral windows were recorded with center photon energies of 1370, 1259, and 1165 cm^{-1}. The averaged and aligned spectra are drawn as bold lines, and the underlying data sets are drawn as gray lines. (c) Difference spectra at two delay times after photoexcitation. The spectrum denoted as "650 fs" is the average over all of the spectra from 500 to 800 fs, and the spectrum denoted as "6.5 ps" is integrated from 3 to 10 ps. (d) Kinetics at the wavenumbers as indicated. The kinetics are integrated over ±3 cm^{-1}.

Simple Method for ^{18}O Labeling of Amino Acids. Labeling of the backbone carbonyl function as ^{13}C═^{18}O is particularly important for probing the amide I region of infrared spectra.[39] The amide I vibrations give rise to strong absorption peaks at approximately 1640 cm^{-1}, and the introduction of ^{13}C═^{18}O labels results in an approximately 60 cm^{-1} red shift that enables spectral isolation.[39] Unfortunately, ^{13}C═^{18}O-labeled amino acids are generally not commercially available. Synthesis from ^{13}C-labeled precursors may be achieved by refluxing the compound in a water-free dioxane/$H_2{}^{18}O$ mixture at acidic pH.[40] We applied a simplified procedure for ^{18}O labeling of the backbone carbonyl in the synthesis of compound **9**. The exchange was performed under acidic conditions by addition of 4 M HCl in 1,4-dioxane to the amino acid derivative premixed with ^{18}O-enriched water in 1,4-dioxane under a nitrogen atmosphere (Figure 3b and Supplementary Scheme 2). The reaction mixture was heated to 100 °C using an oil bath in a sealed microwave vial overnight. LC−MS analysis confirmed quantitative ^{18}O labeling within 20 h (see the Supporting Information for analytical data). In contrast to

DOI: 10.1021/jacs.5b12680
J. Am. Chem. Soc. 2016, 138, 2312−2318

earlier reports, with this method neither in situ generation of HCl gas[18,40] nor repetition of the reaction is necessary for full conversion.

Isotope-Edited Infrared Spectroscopy. We used our isotope-labeling method to unambiguously assign the fingerprint vibrations in difference infrared spectra of tyrosine 66 in GFP. Tyr66 is part of the chromophore and deprotonates upon photoexcitation within a few picoseconds. The proton is transferred past a water molecule and a serine side chain to glutamate 222.[8,41,42] We targeted the 1100 to 1400 cm^{-1} fingerprint region of the infrared spectrum. While this spectral range contains a wealth of information on chemical structure and dynamics, the features are also notoriously difficult to assign.[3]

To guide the protein synthesis, we calculated the spectral shifts of different isotope-labeling patterns on the tyrosine using density functional theory (DFT) calculations. While DFT calculations are usually not very reliable in predicting the peak positions of fingerprint vibrations, the computation of isotope shifts should be much more robust. Replacing all of the carbons in the phenyl ring by ^{13}C (Tyr-$^{13}C_6$) produced the largest predicted shift (Figure 4a). We therefore synthesized GFPcyc3$^{Tyr66\text{-}^{13}C_6}$ on a preparative scale and purified it by affinity chromatography (Figure 2d). From 100 mL of cell-free reaction, 1.6 mg of purified and concentrated GFPcyc3$^{Tyr66\text{-}^{13}C_6}$ was obtained, which corresponds to about 13% of the $tRNA_{CUA}^{Tyr\text{-}^{13}C_6}$ incorporated into the purified protein.

This sample was subjected to UV pump−infrared probe difference spectrometry using our home-built setup (see Methods for details). GFP was photoexcited using laser pulses centered at 400 nm. Infrared difference spectra from 1426 to 1117 cm^{-1} are shown in Figure 4b for the labeled GFP (red line) and for a wild-type GFP sample (black line). Inspection of these spectra reveals that the positions of the positive peaks at 1375 and 1188 cm^{-1} and the negative peaks at 1292, 1174, and 1152 cm^{-1} are red-shifted in the isotope-labeled sample. We conclude that these peaks must be due to side-chain vibrations of Tyr66. The assignment also allows us to conclude that the negative peak at 1240 cm^{-1} does not originate from the Tyr66 residue. This peak is likely caused by a different amino acid participating in the photoreactions of GFP.

We also performed DFT computations on the truncated chromophore. DFT calculations are often used to aid assignment of infrared spectra, but the computed absolute spectral positions usually carry a significant uncertainty. This was also the case for our calculations, and we adjusted the wavenumber scales by a constant factor to match the wild-type spectrum. When it comes to predicting isotope-induced spectral shifts, DFT should be much more robust because the influence of the increased masses of the isotopes on the reduced masses for the vibrations can be estimated with precision. Indeed, the predicted isotope shifts agree with the observed shifts (Figure 4a,b).

With the tyrosine peaks assigned on the basis of isotope-induced spectral shifts, we now inspect the peak at 1375 cm^{-1} more closely. The peak converts from a double peak at early times after photoexcitation (650 fs; Figure 4c) into a single peak (6.5 ps; Figure 4c). The conversion has a characteristic time constant of 3 ± 1 ps (Figure 4d), and the final spectral shape is stable for >1 ns (data not shown). We interpret this conversion to be a sign of deprotonation of the chromophore.[43] Directly after photoexcitation, the chromophore relaxes in its electronically excited, protonated state, and after 3 ps the proton departs from the phenol OH group, leaving the tyrosinate behind.[8]

DISCUSSION

We have demonstrated that the active site of a protein can be site-specifically isotope-labeled in sufficient yields to perform time-resolved infrared spectroscopy. The production yield in our cell-free system (75 μg of protein/mL of reaction mixture) was limited by the concentration of aminoacylated tRNA (Supporting Figure 1 and Figure 2c). This compound has to be chemically synthesized for each amino acid and is also the most expensive reactant. The overall material cost of a labeled protein was approximately 6000 dollars/mg of protein. The T4 RNA ligase 1 (New England Biolabs) and the pdCpA (ATDBio), which are needed in the synthesis of the aminoacylated tRNA, are the main cost drivers. It would therefore be interesting to explore alternative methods for more efficient production of the aminoacylated tRNA.

With the label in place, we were readily able to assign peaks in the infrared difference absorption spectra to specific amino acid vibrations while conserving the functionality of the wild-type protein. Previously these assignments were not possible, despite the abundance of knowledge about the GFP photocycle,[8,41,42] spectroscopic experience,[3] and highly developed computational methods. Specific isotope labeling, as demonstrated here, enabled the spectral interpretation. If the three-dimensional structure of a protein is known, such definite assignments add a spatial dimension to infrared spectroscopy.

The fingerprint region of the infrared spectrum yields highly specific information. This is illustrated by the spectral evolution of the peak at 1375 cm^{-1} (Figure 4c,d). From this peak we find that the deprotonation of Tyr66 occurs after a few picoseconds of dwell time, which confirms earlier proposals.[8,22] The deprotonation could be limited by additional structural rearrangements of the protein or the chromophore. However, the dwell time could also reflect the tunneling barrier of the protons. The latter suggestion is supported by the lengthening of the proton relay time when the protons are exchanged for deuteriums.[8,41] It is conceivable that our method can be used to deduct specific information about transient states in other photoactive proteins, such as photoreceptor proteins or photosynthetic proteins.

In this work, we have used isotope-induced shifts to assign absorption peaks in *difference* infrared spectra. However, isotope shifts can also be used to isolate peaks in *absolute* spectra. This has, for example, been exploited to study the aggregation behavior of amyloids[17] and unfolding of peptides[19] with multidimensional infrared spectroscopy. With the method presented in this paper, larger proteins could in principle be studied in a similar way. Whether the desired peaks can be isolated requires further investigation because spectral crowding becomes increasingly restrictive with protein size. Also, it is often not easy to predict how the excitonic coupling of amide groups would be changed by isotope labeling of one specific site. Nevertheless, experiments that require site-specific isotope labeling of larger proteins have been suggested. One intriguing idea is to determine the ion occupancy[44] in the selection filter of the ion channel KcsA with two-dimensional spectroscopy.[35]. This proposed experiment has not yet been performed because site-selective isotope labeling of the protein was not possible. The method presented here can open this bottleneck.

DOI: 10.1021/jacs.5b12680
J. Am. Chem. Soc. 2016, 138, 2312−2318

METHODS

Wild-Type GFP. Wild-type GFP was produced by cloning GFPcyc3[45] into the vector pIVEX2.4d[33] (Roche Applied Science) and heterologous expression in *E. coli* BL21 Star (DE3) (Invitrogen). Purification was by Ni^{2+}-affinity chromatography (Ni-NTA agarose, Quiagen).

Extract Preparation and RF1 Depletion. S12 extract was prepared from BL21 (DE3):RF1−$(CBD)_3$[31] as described by Pedersen.[33] To remove RF1, the S12 extract was passed over chitin resin (New England Biolabs) directly after the incubation, and the removal was confirmed by Western blotting (Figure 2a). After the addition of 1 mM DTT, the S12 extract was dialyzed twice against extract buffer supplemented with β-mercaptoethanol (1 mL/L), flash-frozen, and stored at −80 °C.

Cell-Free Protein Expression. Cell-free protein expression was performed in batch mode as described previously.[33] For every batch of S12 extract, the optimal Mg^{2+} was determined by maximizing the GFP fluorescence at 520 nm. To prepare tRNA(-CA)$^{AA*^{NVOC/NB}}_{CUA}$, aminoacylated pdCpA (**1**−**15**) was synthesized as described in Extended Methods in the Supporting Information (SI) and coupled to tRNA(-CA)$_{CUA}$, prepared by runoff transcription,[46,47] by using T4 RNA ligase 1[48] (New England Biolabs). Deprotection of ∼25 μM tRNA(-CA)$^{AA*^{NVOC/NB}}_{CUA}$ was done at acidic pH and 2 °C at a volume of 400 μL in a 1.5 mL in a Protein LoBind tube (Eppendorf, serves as an additional high-pass (HP) filter (>320 nm)). The sample was illuminated for 10 min using a 500 W Xe lamp equipped with a water filter and a 320 nm HP filter (Schott). After exposure, samples were immediately flash-frozen, stored at −80 °C, and used without further purification. Deprotection of ∼25 μM tRNA(-CA)$^{AA*^{pentenoyl}}_{CUA}$ was achieved by treating the suppressor tRNA with 5 mM iodine (10% v/v tetrahydrofuran) for 45 min at 25 °C. After deprotection, 0.3 M NaOAc (pH 5.2) was added, and tRNA(-CA)$^{AA}_{CUA}$ was precipitated using isopropanol, resuspended in 1 mM NaOAc (pH 4.5), and stored at −80 °C.

Isotope Labeling. Details of the synthesis are provided in the SI.

DFT Calculations. DFT calculations were performed on a system comprising the GFP chromophore and a coordinating water molecule in the gas phase with the TURBOMOLE 6.6 software package. More details can be found in the SI.

Pump−Probe Spectroscopy. For time-resolved pump−probe infrared spectroscopy, the sample was excited using the second harmonic (400 nm, diameter of ∼120 μm, 250 nJ/pulse) of a mode-locked femtosecond Ti:sapphire amplifier (Spitfire Ace, Spectra-Physics) at a repetition rate of 5 kHz and probed using an infrared pulse generated by a Topas Twin (Light Conversion Ltd.) and non-collinear difference frequency generation (approximately 3 nJ/pulse and a diameter of ∼180 μm at the sample position). In a first set of experiments (Figure 4b), the excitation beam was passed through a 10 cm long glass rod (15 mm aperture, 100 mm length, high NA hexagonal light pipe) to stretch the pulse to a duration of approximately 2 ps. A second set of experiments (Figure 4c,d) was performed using femtosecond pulses with a duration of approximately 100 fs. Reference probe pulses, which were note-guided through the sample, were used to correct for shot-to-shot laser fluctuations. An iHR 320 spectrometer (Horiba) equipped with a grating (5 grooves/mm, 8000 nm blaze wavelength, Horiba) and two 64-element mercury cadmium telluride detector arrays (MCT-8-2 × 64, Infrared Associates) with associated digitizing software (Infrared System Development Corporation, FPAS 0144) were used for detection. To limit photodegradation, the sample was moved perpendicular to the probe beam direction over a total area of ∼1.1 cm^2 using two linear stages in an *xy* configuration (4218S-04-01R0, Newmark).

ASSOCIATED CONTENT

Supporting Information

The Supporting Information is available free of charge on the ACS Publications website at DOI: 10.1021/jacs.5b12680.

Extended methods, reaction schemes, ^1H and ^{13}C NMR spectra, circular dichroism spectra, and HPLC (ESI^+/ESI^-/UV) data (PDF)

AUTHOR INFORMATION

Corresponding Authors

*peukers@gmail.com

*westenho@chem.gu.se

Notes

The authors declare no competing financial interest.

ACKNOWLEDGMENTS

This work was supported by the Knut and Alice Wallenberg Foundation (Sweden), the Swedish Research Council, the Foundation for Strategic Research (Sweden), and the European Research Council. We thank Jean-Michel Betton and Cordula Jany for providing the GFP cycle 3 vector, Sidney Hecht for providing the pYRNA8 vector, and Gabriela Kovácsová for providing the blot in Figure 2d. Ashley Hughes and Matthijs Panman are acknowledged for critical reading of the manuscript. We thank Linnea Isaksson for help with the additional assay (Supporting Figure 1).

REFERENCES

(1) Henzler-Wildman, K.; Kern, D. *Nature* **2007**, *450* (7172), 964.

(2) Vinson, V. J. *Science (Washington, DC, U. S.)* **2009**, *324* (5924), 197.

(3) Barth, A. *Biochim. Biophys. Acta, Bioenerg.* **2007**, *1767* (9), 1073.

(4) Hamm, P.; Lim, M. H.; Hochstrasser, R. M. *J. Phys. Chem. B* **1998**, *102* (31), 6123.

(5) Kolano, C.; Helbing, J.; Kozinski, M.; Sander, W.; Hamm, P. *Nature* **2006**, *444* (7118), 469.

(6) Zheng, J.; Kwak, K.; Asbury, J.; Chen, X.; Piletic, I. R.; Fayer, M. D. *Science* **2005**, *309* (5739), 1338.

(7) Zhao, W.; Wright, J. C. *Phys. Rev. Lett.* **1999**, *83* (10), 1950.

(8) Fang, C.; Frontiera, R. R.; Tran, R.; Mathies, R. A. *Nature* **2009**, *462* (7270), 200.

(9) Deng, H.; Callender, R. In *Infrared and Raman Spectroscopy of Biological Materials*; Gremlich, H.-U., Yan, B., Eds.; Marcel Dekker: New York, 2001; pp 477−514.

(10) King, J. T.; Kubarych, K. J. *J. Am. Chem. Soc.* **2012**, *134* (45), 18705.

(11) Waegele, M. M.; Culik, R. M.; Gai, F. *J. Phys. Chem. Lett.* **2011**, *2*, 2598.

(12) Liu, C. C.; Schultz, P. G. *Annu. Rev. Biochem.* **2010**, *79*, 413.

(13) Ye, S. X.; Zaitseva, E.; Caltabiano, G.; Schertler, G. F. X.; Sakmar, T. P.; Deupi, X.; Vogel, R. *Nature* **2010**, *464* (7293), 1386.

(14) Bazewicz, C. G.; Lipkin, J. S.; Smith, E. E.; Liskov, M. T.; Brewer, S. H. *J. Phys. Chem. B* **2012**, *116* (35), 10824.

(15) Schultz, K. C.; Supekova, L.; Ryu, Y.; Xie, J.; Perera, R.; Schultz, P. G. *J. Am. Chem. Soc.* **2006**, *128* (43), 13984.

(16) Getahun, Z.; Huang, C.-Y.; Wang, T.; De León, B.; DeGrado, W. F.; Gai, F. *J. Am. Chem. Soc.* **2003**, *125* (2), 405.

(17) Middleton, C. T.; Marek, P.; Cao, P.; Chiu, C.; Singh, S.; Woys, A. M.; de Pablo, J. J.; Raleigh, D. P.; Zanni, M. T. *Nat. Chem.* **2012**, *4* (5), 355.

(18) Middleton, C. T.; Woys, A. M.; Mukherjee, S. S.; Zanni, M. T. *Methods* **2010**, *52* (1), 12.

(19) Ihalainen, J. A.; Paoli, B.; Muff, S.; Backus, E. H. G.; Bredenbeck, J.; Woolley, G. A.; Caflisch, A.; Hamm, P. *Proc. Natl. Acad. Sci. U. S. A.* **2008**, *105* (28), 9588.

(20) Smith, A. W.; Lessing, J.; Ganim, Z.; Peng, C. S.; Tokmakoff, A.; Roy, S.; Jansen, T. L. C.; Knoester, J. *J. Phys. Chem. B* **2010**, *114* (34), 10913.

(21) Schwans, J. P.; Sunden, F.; Gonzalez, A.; Tsai, Y.; Herschlag, D. *Biochemistry* **2013**, *52* (44), 7840.

DOI: 10.1021/jacs.5b12680
J. Am. Chem. Soc. 2016, 138, 2312−2318

(22) Stoner-Ma, D.; Jaye, A. A.; Matousek, P.; Towrie, M.; Meech, S. R.; Tonge, P. J. *J. Am. Chem. Soc.* **2005**, *127* (9), 2864.
(23) Decatur, S. M. *Acc. Chem. Res.* **2006**, *39* (3), 169.
(24) Remorino, A.; Korendovych, I. V.; Wu, Y. B.; DeGrado, W. F.; Hochstrasser, R. M. *Science (Washington, DC, U. S.)* **2011**, *332* (6034), 1206.
(25) Sonar, S.; Lee, C. P.; Coleman, M.; Patel, N.; Liu, X. M.; Marti, T.; Khorana, H. G.; Rajbhandary, U. L.; Rothschild, K. J. *Nat. Struct. Biol.* **1994**, *1* (8), 512.
(26) Bernhard, F.; Tozawa, Y. *Curr. Opin. Struct. Biol.* **2013**, *23* (3), 374.
(27) Yabuki, T.; Kigawa, T.; Dohmae, N.; Takio, K.; Terada, T.; Ito, Y.; Laue, E.; Cooper, J.; Kainosho, M.; Yokoyama, S. *J. Biomol. NMR* **1998**, *11* (3), 295.
(28) Noren, C. J.; Anthony-Cahill, S. J.; Griffith, M. C.; Schultz, P. G. *Science (Washington, DC, U. S.)* **1989**, *244* (4901), 182.
(29) Ellman, J. A.; Volkman, B. F.; Mendel, D.; Schulz, P. G.; Wemmer, D. E. *J. Am. Chem. Soc.* **1992**, *114* (20), 7959.
(30) Sobhanifar, S.; Reckel, S.; Junge, F.; Schwarz, D.; Kai, L.; Karbyshev, M.; Lohr, F.; Bernhard, F.; Dotsch, V. *J. Biomol. NMR* **2010**, *46* (1), 33.
(31) Loscha, K. V.; Herlt, A. J.; Qi, R. H.; Huber, T.; Ozawa, K.; Otting, G. *Angew. Chem., Int. Ed.* **2012**, *51* (9), 2243.
(32) Isaksson, L.; Enberg, J.; Neutze, R.; Göran Karlsson, B.; Pedersen, A. *Protein Expression Purif.* **2012**, *82* (1), 218.
(33) Pedersen, A.; Hellberg, K.; Enberg, J.; Karlsson, B. G. *New Biotechnol.* **2011**, *28* (3), 218.
(34) Park, H. S.; Hohn, M. J.; Umehara, T.; Guo, L. T.; Osborne, E. M.; Benner, J.; Noren, C. J.; Rinehart, J.; Soll, D. *Science (Washington, DC, U. S.)* **2011**, *333* (6046), 1151.
(35) Robertson, S. A.; Ellman, J. A.; Schultz, P. G. *J. Am. Chem. Soc.* **1991**, *113* (7), 2722.
(36) England, T. E.; Uhlenbeck, O. C. *Nature* **1978**, *275* (5680), 560.
(37) Hecht, S. M. In *Protein Engineering*; Köhrer, C., RajBhandary, U. L., Eds.; Nucleic Acids and Molecular Biology, Vol. *22*; Springer: Berlin, 2009.
(38) Lodder, M.; Golovine, S.; Laikhter, A. L.; Karginov, V. A.; Hecht, S. M. *J. Org. Chem.* **1998**, *63* (3), 794.
(39) Ihalainen, J. A.; Bredenbeck, J.; Pfister, R.; Helbing, J.; Chi, L.; van Stokkum, I. H. M.; Woolley, G. A.; Hamm, P. *Proc. Natl. Acad. Sci. U. S. A.* **2007**, *104* (13), 5383.
(40) Marecek, J.; Song, B.; Brewer, S.; Belyea, J.; Dyer, R. B.; Raleigh, D. P. *Org. Lett.* **2007**, *9* (24), 4935.
(41) van Thor, J. J. *Chem. Soc. Rev.* **2009**, *38* (10), 2935.
(42) Di Donato, M.; van Wilderen, L. J. G. W.; Van Stokkum, I. H. M.; Stuart, T. C.; Kennis, J. T. M.; Hellingwerf, K. J.; van Grondelle, R.; Groot, M. L. *Phys. Chem. Chem. Phys.* **2011**, *13* (36), 16295.
(43) Chattoraj, M.; King, B. A.; Bublitz, G. U.; Boxer, S. G. *Proc. Natl. Acad. Sci. U. S. A.* **1996**, *93* (16), 8362.
(44) Köpfer, D. A.; Song, C.; Gruene, T.; Sheldrick, G. M.; Zachariae, U.; de Groot, B. L. *Science* **2014**, *346* (6207), 352.
(45) Crameri, A.; Whitehorn, E. A.; Tate, E.; Stemmer, W. P. *Nat. Biotechnol.* **1996**, *14* (3), 315.
(46) Gao, R.; Zhang, Y.; Choudhury, A. K.; Dedkova, L. M.; Hecht, S. M. *J. Am. Chem. Soc.* **2005**, *127* (10), 3321.
(47) Robertson, S. A.; Noren, C. J.; Anthony-Cahill, S. J.; Griffith, M. C.; Schultz, P. G. *Nucleic Acids Res.* **1989**, *17* (23), 9649.
(48) England, T. E.; Bruce, A. G.; Uhlenbeck, O. C. *Methods Enzymol.* **1980**, *65* (1), 65.

DOI: 10.1021/jacs.5b12680
J. Am. Chem. Soc. 2016, 138, 2312−2318